

## Spectral characteristics of the integral operator of the internal problem of electrodynamics for elliptical frame structure

Dmitry P. Tabakov, Andrey G. Mayorov

Povolzhskiy State University of Telecommunications and Informatics

23, L. Tolstoy Street,  
Samara, 443010, Russia

*Abstract* – The article is devoted to the analysis of electrodynamic properties elliptical frame structure. Taking into account double symmetry internal problem of electrodynamics for the structure under consideration in the framework of the thin-wire approximation is reduced to four integral Fredholm equations of the first kind, written with respect to independent current functions. A study of spectral characteristics of the integral operators of the corresponding integral equations for various values of the electrical length and ellipticity of the frame. It is shown that the eigenfunctions of integral operators for close values of these parameters have a high degree of correlation, with In this case, the eigenfunctions are close in form to trigonometric functions. Features of the frequency dependence of the eigenvalues integral operators. The conclusion is made about the resonant nature of these dependences, what makes an elliptical frame structure in many respects similar to the previously considered tubular vibrator and spherical spiral particle. The results presented in the article form an in-depth understanding of the processes occurring in the structure under consideration, and also serve as a guideline in the construction of approximation models for solving the internal tasks.

*Keywords* – elliptical loop structure; loop antenna; integral representation of the electromagnetic field; current distribution; integral equation; eigenfunctions; eigenvalues.

### Introduction

Loop antennas are one of the most common types of antennas, and they have several applications (television, cellular communications, radio communications, etc.). Theoretical research on loop antennas has been conducted for quite a long time; hence, a rather large number of scientific works on this subject now exist. At present, the characteristics of such structures can be calculated with a high degree of accuracy using computer-aided design systems, engineering equations, and developed models of other works that have varying degrees of complexity. In [1], a loop antenna is examined in the approximation of the uniform current distribution. In [2], the long-line theory is applied for the calculations. In [3; 4], in the cross section of a conductor with small wave sizes, a quasistatic approximation is introduced for the current distribution. In [5], a ring stripline antenna is considered, for which an infinite set of integral equation systems (IESs) are developed with respect to the Fourier harmonics of the components of the surface current density vector on the strip. The obtained results allow estimation of the relationship between the amplitudes of the longitudinal and transverse current components.

It is worthy to note that rigorous mathematical models have been designed mostly only for ring frames with the simplest geometry. The axial symme-

try of the structure present in this case significantly simplifies the solution of the interior problem. Rigorous models of frames of more complex configurations (e.g., elliptical, polygonal) are not so common; therefore, developing such mathematical models is urgently needed. Even for rigorous models developed in the form of IE (including singular ones), authors, as a rule, limit themselves to the analysis of the quantitative characteristics of current distributions without investigating the reasons that result in the formation of these distributions. This aspect is critical to producing an adequate pattern of the interior physical processes in the structures being considered. This problem can be solved using the eigenfunction method (EFM) developed in [6]. Previously, this method was applied by the authors to the analysis and construction of an approximation of the interior problem solution for a tubular electric dipole [7; 8]. An alternative to EFM is the characteristic mode method [9–11]. Its advantages over EFM are the simplicity of the numerical implementation; however, a significant disadvantage of this method is the low stability of the computational procedure.

We discuss a mathematical model of an elliptical frame (EF) structure expressed in the form of four independent IEs. The solution to the interior electrodynamic problem is developed on the basis of EFM. The method of EF excitation was not specified to increase the generality of the presented results, i.e., the devel-

oped model can be employed to solve both antenna and diffraction problems. In a given frequency range for different variants of the EF geometry, the spectral characteristics of the integral operators of the corresponding IEs were analyzed.

## 1. Statement of the problem

Consider solving the interior problem of electrodynamics on an EF structure using the eigenfunction method. The geometry of the structure is shown in Fig. 1. An EF conductor, which has infinitely high conductivity, has a circular cross section with a diameter  $2\varepsilon$ , which is much less than the wavelength  $\lambda$  and the total length  $L$  of the conductor generatrix. Therefore, for EF, it is desirable to utilize the thin-wire approximation, within which the volumetric current density is decreased to the azimuthally independent total current flowing along the conductor generatrix. Hereafter, the symbol  $L$  denotes a generatrix.

The parametric equation of the EF generatrix  $L$  has the form

$$\mathbf{r}(t) = r_x \cos t \mathbf{x} + r_y \sin t \mathbf{y}, \quad t \in [0; 2\pi]. \quad (1)$$

Here,  $t$  is the azimuth of a cylindrical or spherical coordinate system and  $r_x$  and  $r_y$  are the major and minor semiaxes of the ellipse, respectively. The natural parameter on the spirals is calculated using

$$l(t) = \int_0^t \left| \frac{d\mathbf{r}(t)}{dt} \right| dt' = r_x \int_0^t \sqrt{\sin^2 t' + \kappa \cos^2 t'} dt', \quad (2)$$

Here,  $\kappa = r_y / r_x \leq 1$  is the ellipticity coefficient. In the natural parameter, the equation of the generatrix of the spiral is obtained using Eq. (1) after  $t = t(l)$ . The function  $t(l)$  is determined numerically from Eq. (2) by the inverse interpolation method. The length of the EF generatrix is described as  $L = l(2\pi) = 4r_x E(\sqrt{1 - \kappa^2})$ , where  $E(x)$  is a complete elliptic integral of the second kind [12]. The radius of curvature  $\rho_{\min}$  of the EF generatrix  $L$  has a minimum value at points that correspond to  $t = 0$  and  $t = \pi$ :  $\rho_{\min} = r_x \kappa$ . This equality needs the imposition of an additional condition on the radius of the conductor  $\varepsilon \ll r_x \kappa$ .

Within the adopted model, the EFM structure is described by an integral representation (IR), described in detail in [13]:

$$\mathbf{F}(\mathbf{r}) = \int_L I(l') \mathbf{K}^{(F)}(\mathbf{r}, \mathbf{r}(l')) dl', \quad F \equiv E, H; \quad (3)$$

Here,  $\mathbf{K}^{(F)}$  are kernels of the integral representation,  $I(l)$  is the total current distribution on the generatrix of the conductor, and  $\mathbf{r}$  is the radius vector of the observation point. The correctness and reliability of the

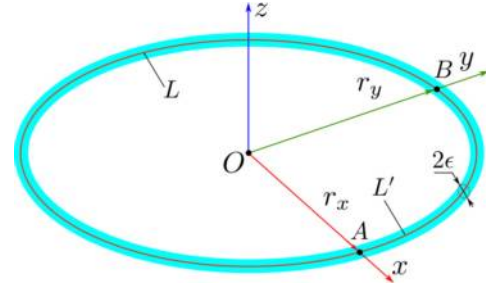


Fig. 1. Thin-wire model of an elliptical frame antenna  
 Рис. 1. Тонкопроволочная модель эллиптической рамочной антенны

results obtained using EFM IR of Eq. (4) are verified in [14; 15].

The structure under consideration with  $\kappa < 1$  has double mirror symmetry relative to the planes  $XOZ$  and  $YOZ$ ; therefore, it can be divided into four identical parts, which generatrices  $L_n \equiv L'$ , and described by general equations

$$\mathbf{r}_n(t) = s_n^{(x)} r_x \cos t \mathbf{x} + s_n^{(y)} r_y \sin t \mathbf{y},$$

$$t \in [0; \pi/2], \quad n = 1 \dots 4.$$

$$\{s_1^{(x)}, s_1^{(y)}\} = \{1, 1\}; \quad \{s_2^{(x)}, s_2^{(y)}\} = \{-1, 1\};$$

$$\{s_3^{(x)}, s_3^{(y)}\} = \{-1, -1\}; \quad \{s_4^{(x)}, s_4^{(y)}\} = \{1, -1\};$$

In this case,

$$\mathbf{F}(\mathbf{r}) = \sum_n \int_{L'} I_n(l') \mathbf{K}^{(F)}(\mathbf{r}, \mathbf{r}_n(l')) dl', \quad (4)$$

$$F \equiv E, H; \quad n = 1 \dots 4.$$

Here,  $I_n(l)$  is the current distribution of the corresponding generatrix. Let us set the following boundary condition

$$(E^{(in)}(\mathbf{r}(l)) + E(\mathbf{r}(l))) \cdot \mathbf{l}(l) = 0$$

on each generatrix, and thus, the following IE system is obtained

$$\sum_{n=1}^4 \int_{L'} I_n(l') K_{m,n}(l, l') dl' = E_m(l),$$

$$m = 1 \dots 4, \quad l \in L' = L/4.$$

Here,

$$E_m(l) = -\mathbf{l}_m(l) \cdot E^{(in)}(\mathbf{r}_m(l)), \quad (5)$$

$$K_{m,n}(l, l') = \mathbf{l}_m(l) \cdot \mathbf{K}^{(E)}(\mathbf{r}_m(l), \mathbf{r}_n(l'))$$

are the tangential components of the external electric field on the generatrices and kernels of the IE system, respectively. Due to the symmetry of the structure, we obtain the following equations:

$$K_{m,m} = K_1, \quad K_{m,5-m} = K_4, \quad m = 1 \dots 4;$$

$$K_{1,2} = K_{2,1} = K_{3,4} = K_{4,3} = K_2;$$

$$K_{1,3} = K_{3,1} = K_{2,4} = K_{4,2} = K_3.$$

For functions  $E_m$ ,  $I_m$ , and  $K_m$ , the following transformations are valid:

$$F_m = \frac{1}{2} \sum_{n=1}^4 w_{m,n} \dot{F}_n, \quad (6)$$

$$\dot{F}_m = \frac{1}{2} \sum_{n=1}^4 w_{m,n} F_n, \quad F \equiv E, I, K,$$

where  $w_{m,n}$  are the elements of the Walsh matrix:

$$\mathbf{W} = \begin{pmatrix} 1 & 1 & 1 & 1 \\ 1 & 1 & -1 & -1 \\ 1 & -1 & -1 & 1 \\ 1 & -1 & 1 & -1 \end{pmatrix}.$$

Regarding functions  $\dot{E}_m$  and  $\dot{I}_m$ , the original IE system is divided into four independent subsystems:

$$\dot{E}_m(l) = \int_{L'} \dot{I}_m(l')(2\dot{K}_m(l,l'))dl', \quad m = 1 \dots 4, \quad l \in L'. \quad (7)$$

Physically, the planes  $XOZ$  and  $YOZ$  are an electric or magnetic wall for the structure being considered; thus, the following boundary conditions are valid for the functions  $\dot{I}_i$  and their derivatives  $\dot{I}'_i$ :

$$\begin{aligned} \dot{I}'_1(0) = \dot{I}'_1(L') = 0; \quad \dot{I}'_2(0) = \dot{I}'_2(L') = 0; \\ \dot{I}'_3(0) = \dot{I}'_3(L') = 0; \quad \dot{I}'_4(0) = \dot{I}'_4(L') = 0. \end{aligned} \quad (8)$$

We approximate the generatrices  $L_i$  by kinked curves  $L_i^{(N)}$ , having  $N$  segments of equal length  $\Delta$ . Within the method of moments, we employ constant functions within the segment as basis functions and delta functions localized at the center of the segment as test functions. As a consequence, four independent SLAEs are obtained with the general form:

$$\mathbf{Z}\mathbf{I} = \mathbf{E}. \quad (9)$$

where  $\mathbf{Z} = \mathbf{Z}^{(m)}$  are moment matrices with elements  $z_{i,j}^{(m)}$ ,  $\mathbf{I} = \mathbf{I}^{(m)}$  are vectors of complex amplitudes of currents  $I_j^{(m)}$  on segments, and  $\mathbf{E} = \mathbf{E}^{(m)}$  are vectors with the values of external field functions  $E_j^{(m)}$  at the centers of segments

$$z_{i,j}^{(m)} = 2 \int_{l_i^* - \Delta/2}^{l_i^* + \Delta/2} \dot{K}_m^{(N)}(l_i^*, l') dl',$$

$$I_j^{(m)} = I_m(l_j^*), \quad E_j^{(m)} = E_m(l_j^*);$$

Here,  $l_i^* = (l_{i+1} + l_i)/2$  are the values of the natural parameter at the centers of the segments,  $l_i$  are the values of the natural parameter at the boundaries of the segments, and the superscript “ $N$ ” in the kernels  $\dot{K}_m$  refers to that in  $K_{m,n}$  described by the second equation of Eq. (5), and rather than the original

generatrices  $\mathbf{r}_m(l)$ , their linearized approximations  $\mathbf{r}_m^{(N)}(l)$  are applied. Furthermore, if there is no need, the index  $m$  for the matrices and vectors is omitted.

The complete eigenvalue problem (EVP) for a matrix  $\mathbf{Z}$  is expressed as follows:

$$\mathbf{Z}\mathbf{J} = \mathbf{X}\mathbf{J}. \quad (10)$$

In this equation,  $\mathbf{J}$  is a matrix in which columns  $\mathbf{J}_i$  are eigenvectors (EVs) of  $\mathbf{Z}$ , while all EVs have unit norm  $|\mathbf{J}_n| = 1$ ;  $\mathbf{X}$  is a diagonal matrix in which diagonal elements  $\xi_{i,i} = \xi_i \in \mathbf{X}$  are eigenvalues of  $\mathbf{Z}$ . Here, it should be noted that the SLAE of Eq. (9) is equivalent to the IE of Eq. (7) with a degenerate kernel, calculated for segmented generatrices, and the EVs  $\mathbf{J}_n$  approximate the eigenfunctions (EFs)  $J_n(l)$  of the integral operator of the problem of Eq. (7). Solving the complete eigenvalue problem for complex matrices is a standard linear algebra problem that is solved using the QR algorithm [16]. The SLAE solution with known  $\mathbf{J}$  and  $\mathbf{X}$  will have the following form:

$$\mathbf{I} = (\mathbf{J}\mathbf{X}^{-1}\mathbf{J}^T)\mathbf{E}.$$

The index “ $T$ ” is the transpose operation. The matrix  $\mathbf{X}$  is diagonal; therefore, calculating the inverse matrix is not much of a problem. Physically, the study of the dependence of EV and EVP on frequency and structure parameters is of particular interest because they largely determine the nature of the interior problem solution. In addition, these studies are the basis for constructing approximation models of solutions [8].

In our case, the length of the EF generatrix  $L$  should be selected as the main parameter normalized to the wavelength  $\chi = L/\lambda$ . We will use the ellipticity coefficient  $\kappa$  as parameter 2. The normalized parameter 3 is the ratio of the wire radius  $\varepsilon$  to the length of the EF generatrix  $L$ . Due to the conditions listed earlier, it does not have a significant effect on the solution interior problem. Therefore, we assume  $\varepsilon/L = \text{const}$ .

It should also be noted here that with  $\kappa = 1$  EF, it has axial symmetry, and the eigenfunctions of the integral operator can be expressed through a pair of corresponding trigonometric functions. In this case, the form of the eigenfunctions does not depend on  $L/\lambda$ .

## 2. Numerical modeling and analysis of the results

The problem of Eq. (10) was solved in a rectangular area:

$$\mathcal{S}: x \in \underline{x}: [x_{\min}; x_{\max}], \quad \kappa \in \underline{\kappa}: [\kappa_{\min}; \kappa_{\max}].$$

At intervals  $\underline{x}$  and  $\underline{\kappa}$ ,  $N_f$  nodes  $x_f$  and  $N_r$  nodes  $\kappa_r$  were introduced uniformly, respectively, forming in pairs a set of points  $\{x_f, \kappa_r\} \in \mathcal{S}$ . In the calculations, it was assumed that  $x_{\min} = 0,01$ ,  $x_{\max} = 5$ ,  $\kappa_{\min} = 0,5$ ,  $\kappa_{\max} = 1$ ,  $N_f = 500$ ,  $N_r = 11$ .

The number of segments  $N$  during linearization of the generatrix was assumed to be 100, and the ratio  $\varepsilon/L'$  was selected to be equal to  $3/250$  to give the condition  $2\varepsilon \leq \Delta \leq 12\varepsilon$  [17] necessary to provide a stable solution of the SLAE within the selected system of projection functions. In this case,  $\rho_{\min}/L'$  with  $\kappa = 0,5$  is approximately 0,4, which corresponds to the previously stated condition  $\varepsilon \ll \rho_{\min}$ .

Calculation of EVP  $\mathbf{X}$  and EV  $\mathbf{J}$  was conducted using the ZGEEV procedure [18], which is included in the open source library LAPACK [19]. An important aspect when performing range calculations in region  $\mathcal{S}$  is tracking the numbers of EV and EVP [20; 21], since for different values of  $x$  and  $\kappa$ , the ZGEEV procedure places EV and EVP in the returned arrays in different manners. Thus, the direct calculation of EV and EVP in practice must be supplemented with an algorithm for tracking and sorting them as well as an algorithm for correcting the sign of EV. A correlation algorithm was employed to obtain the results of this study. It was also previously used in [6], but unfortunately, it was not described in detail because of the limited scope of the article. In this article, we will fill this gap.

Let  $\mathbf{J}(x_{f^*}, \kappa_{r^*})$  be the EV matrix, which we take as a sample, and  $\mathbf{J}(x_f, \kappa_r)$  be a matrix that needs to be sorted by EV and adjusted from signs. The essential aspect here is the following conditions:

$$2|x_f - x_{f^*}| / |x_f + x_{f^*}| \ll 1; \quad (11)$$

$$2|\kappa_f - \kappa_{f^*}| / |\kappa_f + \kappa_{f^*}| \ll 1,$$

that is, calculations must be conducted for matrices located in close points of region  $\mathcal{S}$ , which guarantees a high degree of EV correlation. For distant points, EVs with the same indices may have a low degree of correlation and a very different shape. To correct the numbers and signs of EV, it is necessary to compute the correlation matrix:

$$\mathbf{K} = \mathbf{J}^T(x_{f^*}, \kappa_{r^*})\mathbf{J}(x_f, \kappa_r).$$

Next, each line  $\mathbf{K}$  is normalized to the element of the corresponding line with the maximum absolute value. After this step, each line  $\mathbf{K}$  will contain one element  $k_{i,j}$ , with a value of 1 or  $-1$ , and the values of the remaining elements under the condition of Eq. (11) will be significantly less than 1 in absolute

value. The column with the index  $i$  of the adjusted matrix  $\mathbf{J}(x_f, \kappa_r)$  will correspond to the  $j$ -th column of the original matrix  $\mathbf{J}(x_f, \kappa_r)$ , multiplied by a scalar  $k_{i,j}$  (sign correction). The position of the element  $k_{i,j}$  is also employed to adjust the numbers of the EVP vector  $\mathbf{X}(x_f, \kappa_r)$  (without adjusting the sign). Here,  $i$  is the position in the adjusted EVP vector, and  $j$  is the position in the original EVP vector. After correction, the matrix  $\mathbf{J}(x_f, \kappa_r)$  can be taken as reference ( $x_f \rightarrow x_{f^*}$ ;  $\kappa_r \rightarrow \kappa_{r^*}$ ) and the procedure can be repeated for the matrix  $\mathbf{J}$ , calculated at a new point in region  $\mathcal{S}$  that meets the condition of Eq. (11).

In our case, the matrix  $\mathbf{J}(x_1, \kappa_1)$  was taken as reference. At stage 1, matrices  $\mathbf{J}(x_1, \kappa_r)$  and vectors  $\mathbf{X}(x_1, \kappa_r)$  were corrected for  $r = 2 \dots N_r$ . At stage 2, the corrected matrices were employed to correct matrices  $\mathbf{J}(x_f, \kappa_r)$  and vectors  $\mathbf{X}(x_f, \kappa_r)$  for the corresponding index  $r$  ( $r = 2 \dots N_f$ ).

Numerical calculations have two aims. The first aim, which has predominantly practical significance, is associated with determining the possibilities of constructing an approximation model for solving an interior problem based on the EFM. To realize this goal, it becomes necessary to solve some tasks. Task 1 includes the analysis of the degree of correlation of EV calculated at various points in region  $\mathcal{S}$ . This information is crucial to determine the possibility of constructing an approximation of the EV matrices in the specified area. Task 2 is associated with the analysis of EF forms  $J_n(l)$ , determined by the result of interpolation of the corresponding columns of matrices  $\mathbf{J}$ , with collocation points  $l_i^*$ , with  $i = 1 \dots N$  acting as interpolation nodes. Based on the findings of this analysis, it is possible to determine the systems of functions that are most suitable for approximating eigenfunctions in the form of corresponding series. Task 3 is associated with the analysis of the EVP behavior in region  $\mathcal{S}$ . This analysis, as in the case of the EV, allows determination of the systems of functions that are most applicable for approximating the EVP for various points of  $\mathcal{S}$ .

The second aim is mainly of theoretical significance and is associated with determining the nature of the frequency dependence of EVP. Earlier in [6; 7], for other structures, it has already been revealed that this dependence has a resonant nature; therefore, the main contribution to the formation of a solution to the interior problem is made by only a small part of EF. In this case, we need confirmation of this fact with some additional details for the structure being considered. To estimate the residual between vector

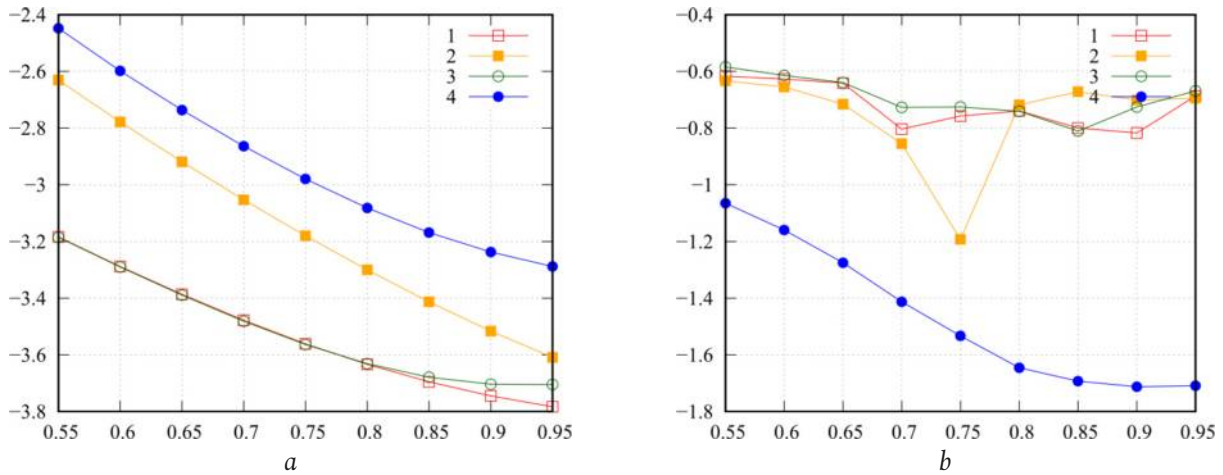


Fig. 2. Dependence  $\rho_r$  on  $\kappa_r^*$ ;  $a - x=0,01$ ;  $b - x=5$ , the number of the curve corresponds to the number of SLE  
 Рис. 2. Зависимость  $\rho_r$  от  $\kappa_r^*$ ;  $a - x=0,01$ ;  $b - x=5$ , номер кривой соответствует номеру СЛАУ

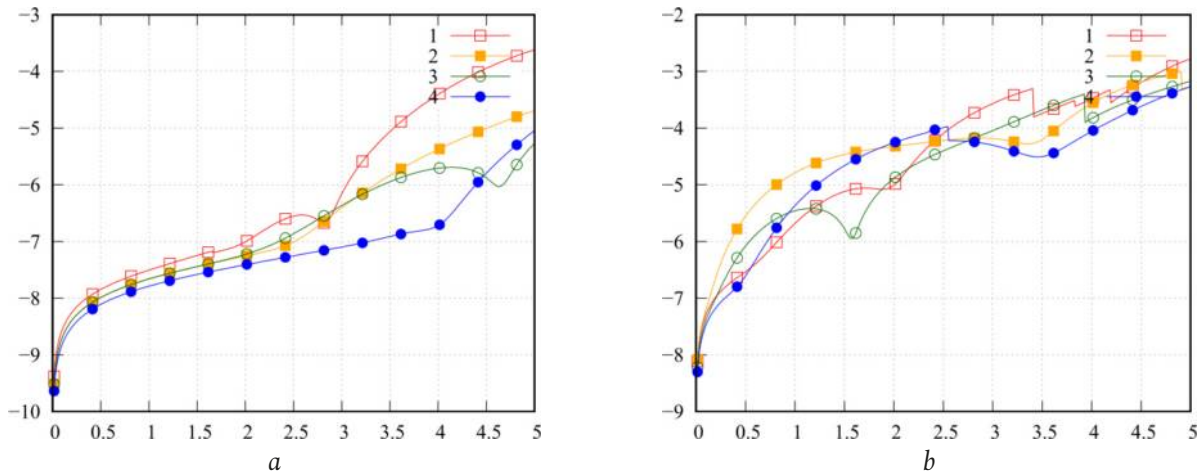


Fig. 3. dependence  $\rho_f$  on  $x_f^*$ ;  $a - \kappa=0,95$ ;  $b - \kappa=0,5$ , the number of the curve corresponds to the number of SLE  
 Рис. 3. Зависимость  $\rho_f$  от  $x_f^*$ ;  $a - \kappa=0,95$ ;  $b - \kappa=0,5$ , номер кривой соответствует номеру СЛАУ

or matrix arrays  $\mathbf{V}$  calculated at a pair of points in region  $\mathcal{S}$ , we use the general equation

$$\text{res}(\mathbf{V}; x^*, \kappa^*; x, \kappa) = \lg \left( 2 \frac{|\mathbf{V}(x^*, \kappa^*) - \mathbf{V}(x, \kappa)|}{|\mathbf{V}(x^*, \kappa^*) + \mathbf{V}(x, \kappa)|} \right).$$

Figure 2 illustrates the graphs of values  $\rho_r = \text{res}(\mathbf{J}; x, \kappa_{r+1}; x, \kappa_r)$  for case  $x=0,01$  (a) and case  $x=5$  (b). The value  $\kappa_r^* = (\kappa_{r+1} + \kappa_r)/2$  is plotted along the abscissa axis. It can be observed that the residual values for different  $m$  differ markedly, while the residual increases with decreasing  $\kappa$  and increasing  $x$ . However, generally, for a rather small value of  $N_r$ , the results can be considered quite good. The residual can be reduced by decreasing the distance between nodes near  $\kappa_{\min}$ . At  $x$  located near  $x_{\max}$ , this will not be sufficient. This also requires an increase in  $N_r$ .

Figure 3 exhibits the graphs of values  $\rho_r = \text{res}(\mathbf{J}; x_{f+1}, \kappa; x_f, \kappa)$  for case  $\kappa=0,95$  (a) and case

$\kappa=0,5$  (b). The value  $x_f^* = (x_{f+1} + x_f)/2$  is plotted along the abscissa axis. Here, it can be observed that the values of the residual are significantly smaller than in the previously considered case, but its spread is also significantly higher, reaching its minimum value at  $x = x_{\min}$  and its maximum at  $x = x_{\max}$ . To reduce the spread of the residual, one should use an uneven arrangement of nodes  $x_f$  the distance between which should decrease with increasing  $x$ . Generally, it should be mentioned that determining the location of control points for a given residual value is an independent and quite interesting computational problem that has application significance.

Figure 4 shows the graphs of values  $\rho_n = \text{res}(\mathbf{J}_n; x_{f+1}, \kappa; x_f, \kappa)$ , detailing the residual on  $x$  for different EV numbers  $n$  at the corner points of region  $\mathcal{S}$ . The SV number is plotted along the abscissa axis. It is clear that the largest contribution to the previously considered residual values is made by EVs with

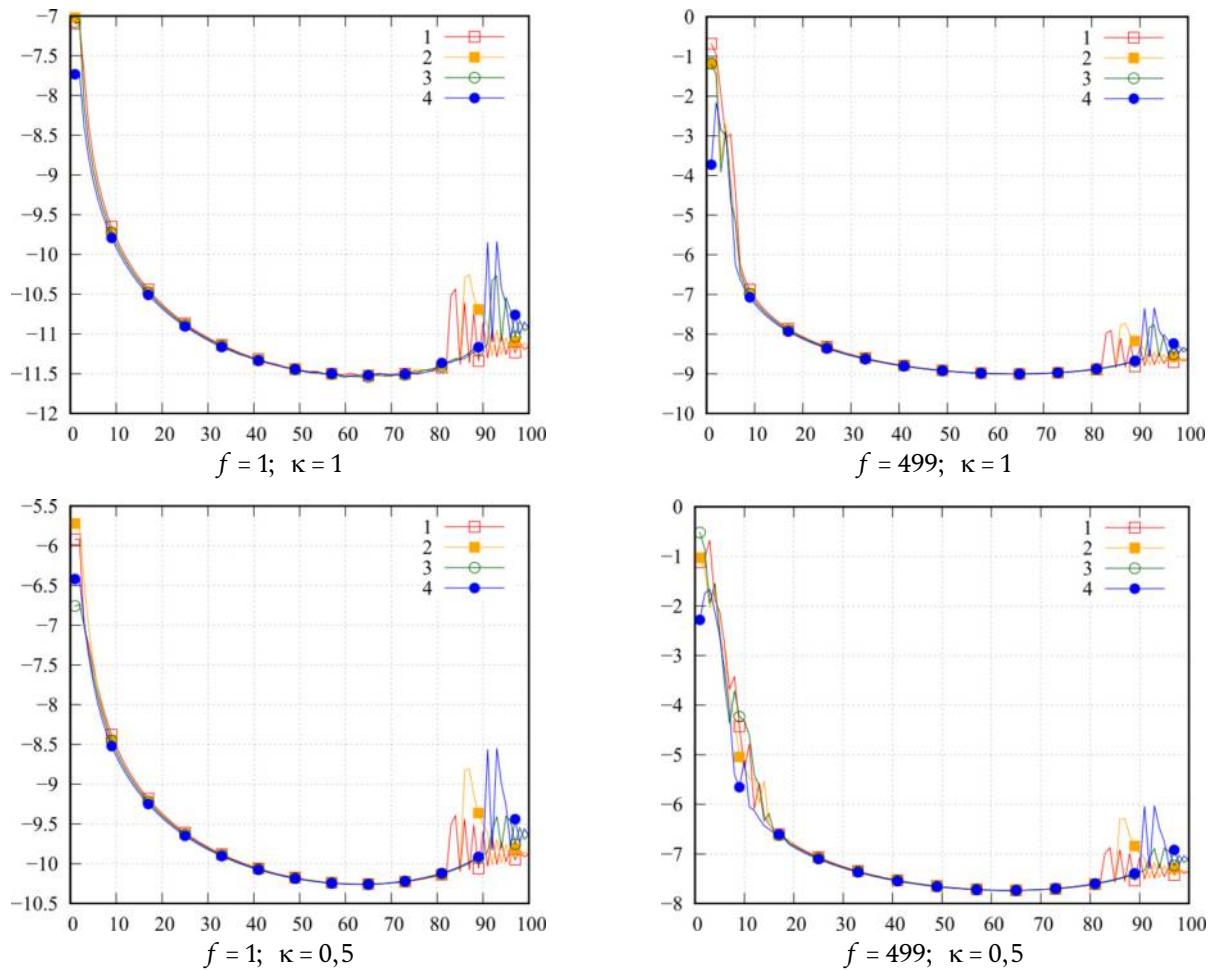


Fig. 4. Dependence  $\rho_n$  on  $n$ , the number of the curve corresponds to the number of SLE  
 Рис. 4. Зависимость  $\rho_n$  от  $n$ , номер кривой соответствует номеру СЛАУ

small  $n$ , which is a good guideline when constructing EV approximations in region  $\mathcal{S}$ .

Figure 5 shows the graphs of the real and imaginary parts of the first four eigenfunctions calculated at  $x = 5$ ,  $\kappa = 0,5$ . It can be observed that they correspond to the conditions of Eq. (8). It is clear that EF can be approximated by rapidly converging series of trigonometric functions. It can also be noted that for  $\kappa = 1$ , the function  $J_1(l)$  has a uniform distribution, and for  $\kappa = 0,5$ , the uniformity is violated, and its maximum shifts to a point with a smaller radius of curvature.

The ratio of the intensities of the real and imaginary parts of the eigenfunctions can be estimated by the magnitude  $\zeta_n(x) = |\text{Im}J_n(x)| / |\text{Re}J_n(x)|$ , and the graphs are shown in Fig. 6. In all cases, a general tendency is observed that at small values of  $x$ , the intensity of the imaginary part of the eigen functions is small; therefore, the oscillations of the EF point occur almost in-phase. As  $x$  increases, the intensity of the real and imaginary parts becomes commensurate, which results in a violation of the in-phase oscillations.

In addition, at large values of  $x$ , there are points at which the intensity of the EF imaginary part is tens of times greater than that of the real part.

Figure 7 shows the graphs of the values  $v'_n(x) = \lg |\zeta_n(x)|$ ;  $v''_n(x) = \arg \zeta_n(x)$  at  $\kappa = 0,5$ . The figure verifies the resonant nature of the behavior of the eigenvalues, while the resonance points can be determined from the condition  $v''_n(x) = 0$ . For  $m = 1, 4$ , medium frequency resonances are registered in the vicinity of even values of  $x$ , while for different  $m$ , the same resonances correspond to EVs, whose indices differ by one. It should separately be noted the nonresonant maximum  $v'_1$  in the vicinity of  $x = 0$  for  $m = 1$ . Also, it is clear that the quality factor of the resonances at  $m = 1$  is slightly higher than that at  $m = 4$  because  $\kappa < 1$ .

An important aspect in the analysis was considering the symmetry, since in the structure under consideration a degeneracy effect is noted, which consists of the coincidence of resonance points for the EVP of matrices of various SLAEs. This effect is

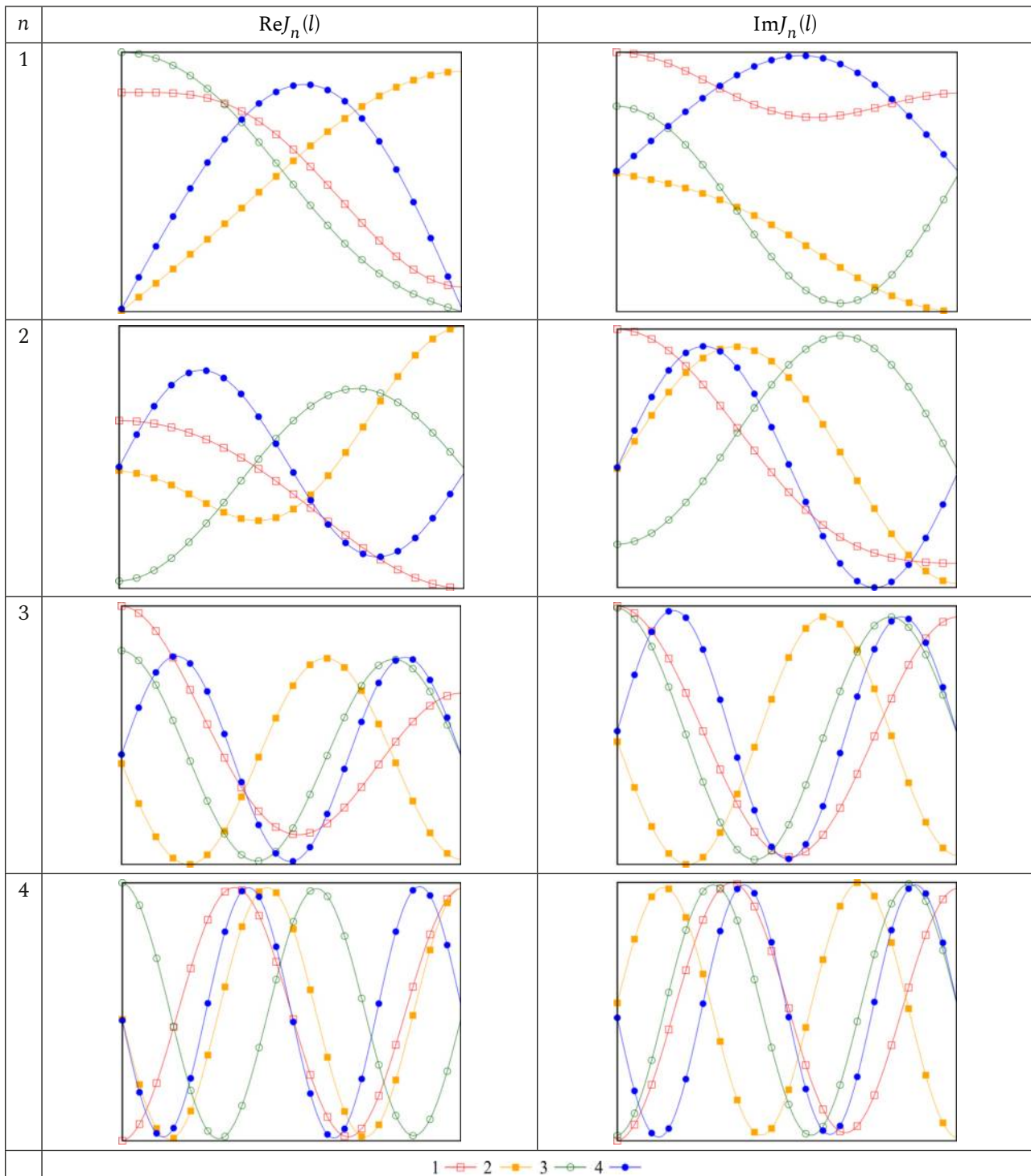


Fig. 5. View of the first four of its own functions  $J_n(l)$ ;  $\chi = 5$ ,  $\kappa = 0,5$ , the curve number corresponds to the number of SLE  
Рис. 5. Вид первых четырех собственных функций  $J_n(l)$ ;  $\chi = 5$ ,  $\kappa = 0,5$ , номер кривой соответствует номеру СЛАУ

noted for  $m = 2,3$ . Meanwhile, it is clear that the corresponding resonances at  $m = 3$  have a higher quality factor because  $\kappa < 1$ .

Generally, we can conclude that the structure under study in terms of the behavior of eigenvalues and the shape of eigenfunctions is in many ways similar to the previously considered tubular dipole [7; 8] and a spherical spiral particle [6]. Thus, the previously

proposed strategies regarding the construction of an approximation model to solve the interior electrodynamic problem are fully applicable to the structure under consideration.

## Conclusion

This study considers a variant of a mathematical model to solve an interior electrodynamic problem for

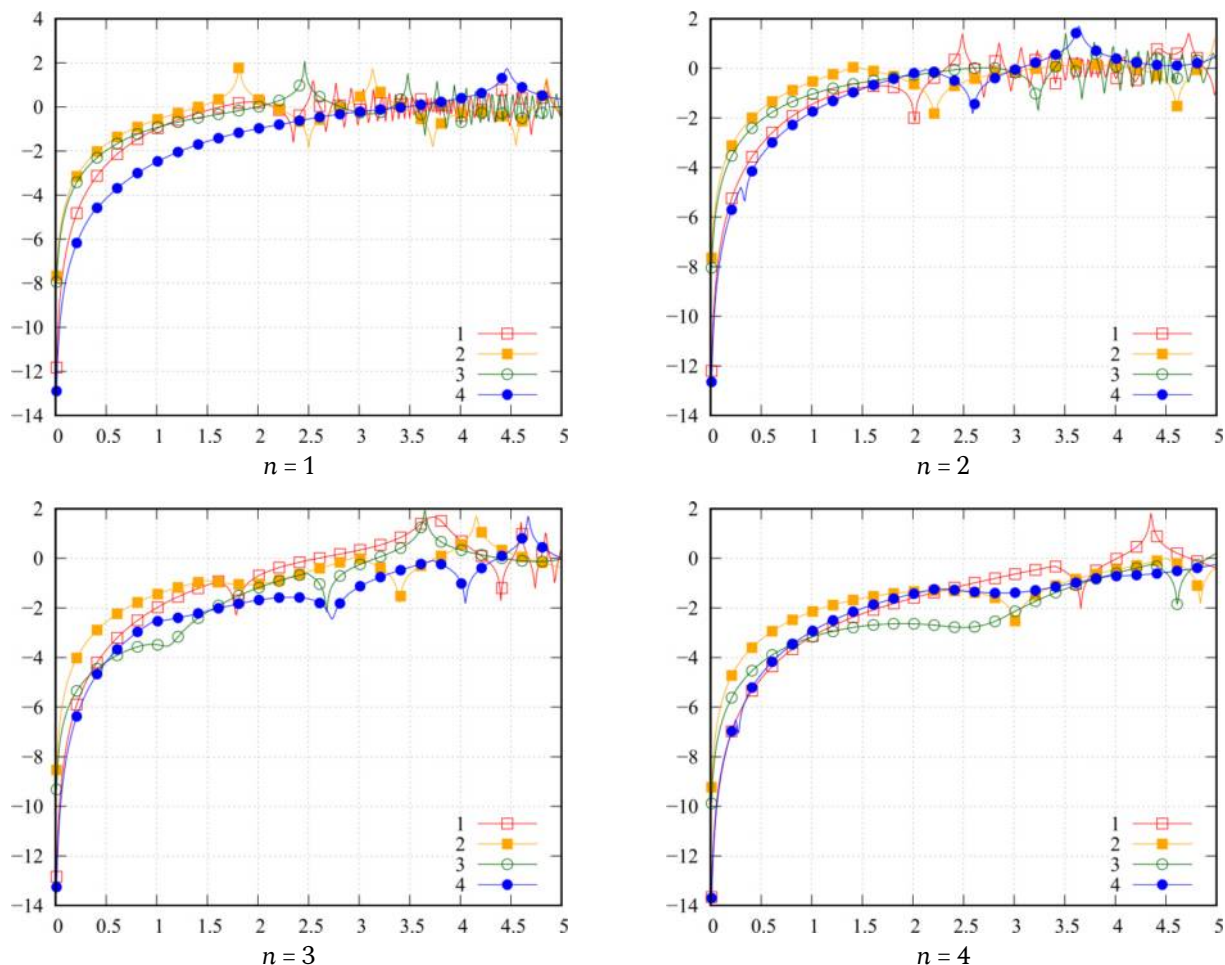


Fig. 6. Dependence  $\zeta_n$  on  $\chi$ ;  $\kappa = 0,5$ , the number of the curve corresponds to the number of SLE  
 Рис. 6. Зависимость  $\zeta_n$  от  $\chi$ ;  $\kappa = 0,5$ , номер кривой соответствует номеру СЛАУ

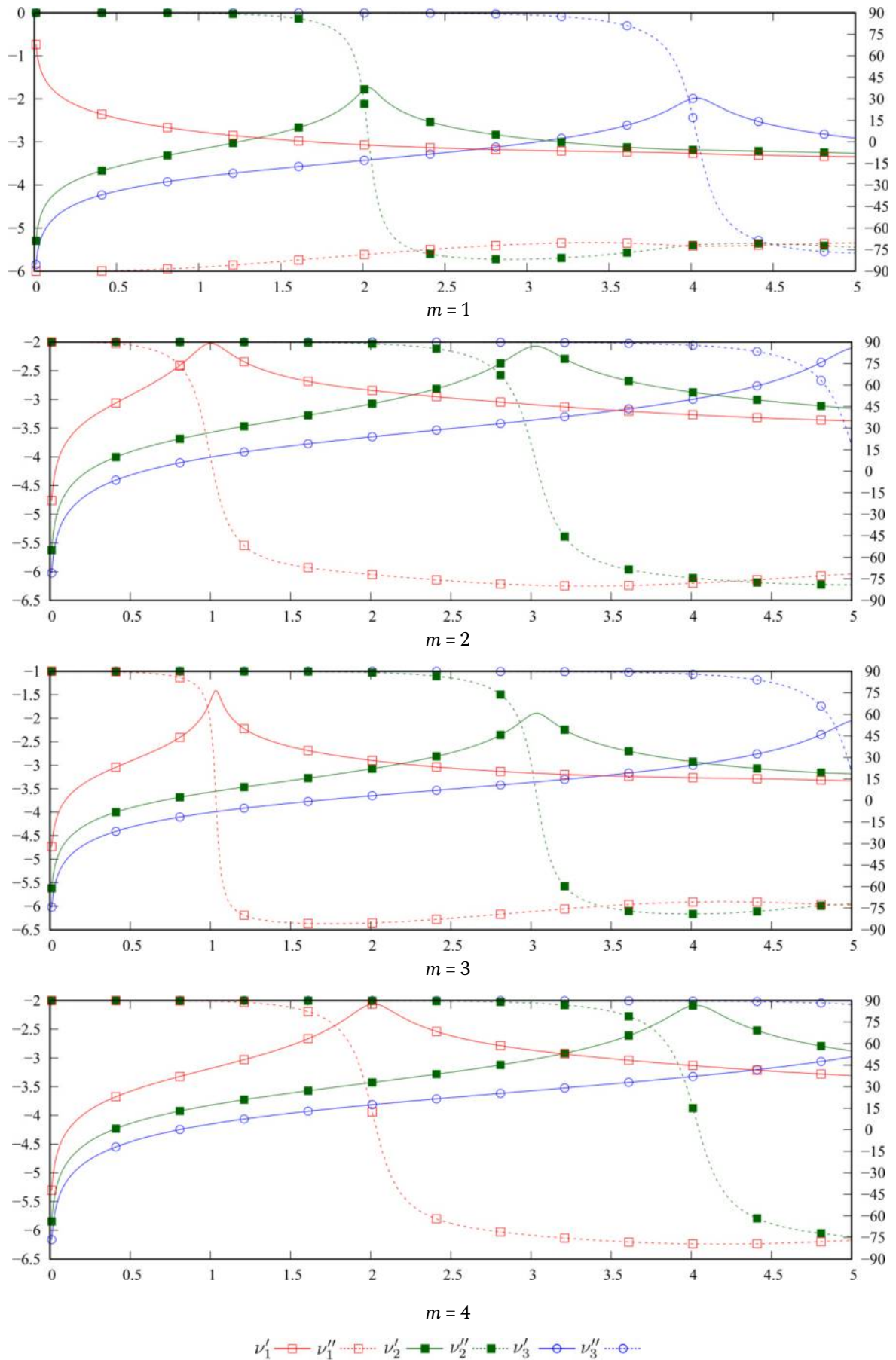
an elliptical spiral structure constructed by thin-wire approximation. The structure has double mirror symmetry, which allows the generation of a mathematical model in the form of four independent Fredholm IEs of the first kind, written relative to the corresponding current functions that meet the boundary conditions for the electric or magnetic wall at the points of intersection of the generatrix of the structure with the symmetry planes. Within the method of moments, the resulting IEs were reduced to SLAEs relative to the values of the current functions on the segments of the linearized generatrix. Solutions of the SLAE are expressed in terms of the eigenvectors and eigenvalues of the SLAE matrix. The eigenvectors of the SLAE approximate the eigenfunctions of the integral operator of the corresponding IE. For each IE, the behavior of the eigenfunctions and eigenvalues of the integral operator was examined depending on the electrical length of the generatrix of the structure and the ellipticity coefficient at a fixed electrically small radius of the conductor.

An estimate of the residual between the eigenfunctions calculated for different values of the specified

parameters is given. It is shown that the discrepancy increases with increasing electrical length of the generatrix of the structure and with decreasing ellipticity coefficient; however, at the selected step of changing the parameters, it has rather small values. A more detailed analysis allowed us to conclude that the most significant contribution to the value of the residual is made by the eigenfunctions of the lower types. This information forms the primary guideline when constructing an approximation model to solve the interior problem of the structure under consideration.

Analysis of the forms of eigenfunctions showed their closeness to trigonometric functions. Therefore, they can be approximated by the corresponding series, which in this case exhibit rapid convergence. In the limiting case, when the ellipse degenerates into a circle, each eigenfunction can be analytically precisely determined by a pair of trigonometric functions.

An analysis of the dependence of the eigenvalues on the electrical length of the generatrix confirmed their resonant nature. Thus, the structure considered

Fig. 7. Dependencies  $v'$  and  $v''$  on  $x$  various values  $m$ ;  $\kappa = 0,5$ Рис. 7. Зависимости  $v'$  и  $v''$  от  $x$  при различных значениях  $m$ ;  $\kappa = 0,5$

from this viewpoint is in many ways similar to the electric dipole and spherical spiral particles previously considered by the authors. That is, it can be argued that a rather limited set of eigenfunctions makes a significant contribution to the solution of the interior problem. It is also worth mentioning here that considering the symmetry of the structure significantly simplifies the numerical analysis when the degeneracy effect occurs, when one eigenvalue can correspond to more than one eigenfunction, which is noted in this case with values of the ellipticity coefficient tending to unity. At lower values of the ellipticity coefficient, only the effect of the degeneration of resonant frequencies is noted.

This work has both theoretical and practical significance. The theoretical significance is related to the development of methods for the electrodynamic analysis of frame emitting and re-emitting structures. The proposed approach offers an in-depth understanding of the behavior of the structures under consideration from the viewpoint of electrodynamics and significantly simplifies the interpretation of the obtained numerical results compared with direct solving of integral equations and their systems. The applied significance is related to the fact that the obtained results can serve as good reference in constructing approximation models to solve the interior problem for the structure under consideration, as well as for structures with similar geometry.

## References

1. Wang T., Bell T. VLF/ELF input impedance of an arbitrarily oriented loop antenna in a cold collisionless multicomponent magnetoplasma. *IEEE Transactions on Antennas and Propagation*, 1972, vol. 20, no. 3, pp. 394–398. DOI: <https://doi.org/10.1109/TAP.1972.1140212>
2. Ohnuki S., Sawaya K., Adachi S. Impedance of a large circular loop antenna in a magnetoplasma. *IEEE Transactions on Antennas and Propagation*, 1986, vol. 34, no. 8, pp. 1024–1029. DOI: <https://doi.org/10.1109/TAP.1986.1143927>
3. Andronov A.A., Chugunov Yu.V. Quasi-stationary electric fields of sources in a rarefied plasma. *UFN*, 1975, vol. 116, no. 5, pp. 79–113. DOI: <https://doi.org/10.3367/UFN.0116.197505c.0079> (In Russ.)
4. Mareev E.A., Chugunov Yu.V. *Plasma Antennas*. Nizhny Novgorod: IPD AN SSSR, 1991, 231 p. (In Russ.)
5. Neganov V.A., Tabakov D.P. The problem of the distribution of the surface current density over a ring strip antenna. *Physics of Wave Processes and Radio Systems*, 2007, vol. 10, no. 4, pp. 8–19. (In Russ.)
6. Tabakov D.P. On the description of radiation and diffraction of electromagnetic waves by the method of eigenfunctions. *Izvestiya vuzov. Radiofizika*, 2021, vol. 64, no. 3, pp. 179–191. URL: <https://radiophysics.unn.ru/issues/2021/3/179> (In Russ.)
7. Tabakov D.P., Mayorov A.G. On the eigenvalues of the integral operator of the singular integral equation of a thin tubular vibrator. *Physics of Wave Processes and Radio Systems*, 2019, vol. 22, no. 1, pp. 26–31. DOI: <https://doi.org/10.18469/1810-3189.2019.22.1.26-31> (In Russ.)
8. Tabakov D.P., Mayorov A.G. Approximation of the solution of an internal electrodynamic problem for a thin tubular vibrator by the method of eigenfunctions. *Trudy uchebnykh zavedeniy svyazi*, 2019, vol. 5, no. 4, pp. 36–42. URL: <https://elibrary.ru/item.asp?id=41664174> (In Russ.)
9. Garbacz R.J. Modal expansions for resonance scattering phenomena. *Proceedings of the IEEE*, 1965, vol. 53, no. 8, pp. 856–864. DOI: <https://doi.org/10.1109/PROC.1965.4064>
10. Harrington R., Mautz J. Theory of characteristic modes for conducting bodies. *IEEE Transactions on Antennas and Propagation*, 1971, vol. 19, no. 5, pp. 622–628. DOI: <https://doi.org/10.1109/TAP.1971.1139999>
11. Harrington R., Mautz J. Computation of characteristic modes for conducting bodies. *IEEE Transactions on Antennas and Propagation*, 1971, vol. 19, no. 5, pp. 629–639. DOI: <https://doi.org/10.1109/TAP.1971.1139990>
12. *Special Functions Reference*. Ed. by M. Abramovitsa, I. Stigana. Moscow: Nauka; Fizmatlit, 1979, 832 p. (In Russ.)
13. Kapitonov V.A. et al. Integral representation of the electromagnetic field of a geometrically chiral structure. *Physics of Wave Processes and Radio Systems*, 2012, vol. 15, no. 4, pp. 6–13. (In Russ.)
14. Tabakov D.P. Thin-wire model of a fractal symmetric vibrator based on Sierpinski's napkin. *Radiotekhnika*, 2015, no. 2, pp. 16–22. (In Russ.)
15. Tabakov D.P., Morozov S.V., Klyuev D.S. Application of the thin-wire integral representation of the electromagnetic field to the solution of the problem of diffraction of electromagnetic waves by conducting bodies. *Physics of Wave Processes and Radio Systems*, 2022, vol. 25, no. 2, pp. 7–14. DOI: <https://doi.org/10.18469/1810-3189.2022.25.2.7-14> (In Russ.)
16. Golub Dzh., Loun Ch. *Matrix Calculations*. Trans. from English. Moscow: Mir, 1999, 548 p. (In Russ.)
17. Strizhkov V.A. Mathematical modeling of electrodynamic processes in complex antenna systems. *Matematicheskoe modelirovanie*, 1989, vol. 1, no. 8, pp. 127–138. URL: <https://www.mathnet.ru/rus/mm/v1/i8/p127> (In Russ.)
18. Интерактивная система просмотра системных руководств (ман-ов) // OpenNET. URL: <https://www.opennet.ru/man.shtml?topic=zgeev&category=3&russian=4>
19. LAPACK // Wikipedia. URL: <https://ru.wikipedia.org/wiki/LAPACK> (In Russ.)
20. Ludick D.J., Jakobus U., Vogel M. A tracking algorithm for the eigenvectors calculated with characteristic mode analysis. *The 8th European Conference on Antennas and Propagation (EuCAP 2014)*, 2014, pp. 569–572. DOI: <https://doi.org/10.1109/EuCAP.2014.6901820>
21. Kalaba R., Spingarn K., Tesfatsion L. Individual tracking of an eigenvalue and eigenvector of a parameterized matrix. *Nonlinear Analysis: Theory, Methods & Applications*, 1981, vol. 5, no. 4, pp. 337–340. DOI: [https://doi.org/10.1016/0362-546X\(81\)90018-3](https://doi.org/10.1016/0362-546X(81)90018-3)

## Список литературы

1. Wang T., Bell T. VLF/ELF input impedance of an arbitrarily oriented loop antenna in a cold collisionless multicomponent magnetoplasma // IEEE Transactions on Antennas and Propagation. 1972. Vol. 20, no. 3. P. 394–398. DOI: <https://doi.org/10.1109/TAP.1972.1140212>
2. Ohnuki S., Sawaya K., Adachi S. Impedance of a large circular loop antenna in a magnetoplasma // IEEE Transactions on Antennas and Propagation. 1986. Vol. 34, no. 8. P. 1024–1029. DOI: <https://doi.org/10.1109/TAP.1986.1143927>
3. Андронов А.А., Чугунов Ю.В. Квазистационарные электрические поля источников в разреженной плазме // УФН. 1975. Т. 116, № 5. С. 79–113. DOI: <https://doi.org/10.3367/UFNr.0116.197505c.0079>
4. Мареев Е.А., Чугунов Ю.В. Антенны в плазме. Нижний Новгород: ИПД АН СССР, 1991. 231 с.
5. Неганов В.А., Табаков Д.П., Задача о распределении поверхностной плотности тока по кольцевой полосковой антенне // Физика волновых процессов и радиотехнические системы. 2007. Т. 10, № 4. С. 8–19.
6. Табаков Д.П. Об описании излучения и дифракции электромагнитных волн методом собственных функций // Известия вузов. Радиофизика. 2021. Т. 64, № 3. С. 179–191. URL: <https://radiophysics.unn.ru/issues/2021/3/179>
7. Табаков Д.П., Майоров А.Г. О собственных значениях интегрального оператора сингулярного интегрального уравнения тонкого трубчатого вибратора // Физика волновых процессов и радиотехнические системы. 2019. Т. 22, № 1. С. 26–31. DOI: <https://doi.org/10.18469/1810-3189.2019.22.1.26-31>
8. Табаков Д.П., Майоров А.Г. Аппроксимация решения внутренней электродинамической задачи для тонкого трубчатого вибратора методом собственных функций // Труды учебных заведений связи. 2019. Т. 5, № 4. С. 36–42. URL: <https://elibrary.ru/item.asp?id=41664174>
9. Garbacz R.J. Modal expansions for resonance scattering phenomena // Proceedings of the IEEE. 1965. Vol. 53, no. 8. P. 856–864. DOI: <https://doi.org/10.1109/PROC.1965.4064>
10. Harrington R., Mautz J. Theory of characteristic modes for conducting bodies // IEEE Transactions on Antennas and Propagation. 1971. Vol. 19, no. 5. P. 622–628. DOI: <https://doi.org/10.1109/TAP.1971.1139999>
11. Harrington R., Mautz J. Computation of characteristic modes for conducting bodies // IEEE Transactions on Antennas and Propagation. 1971. Vol. 19, no. 5. P. 629–639. DOI: <https://doi.org/10.1109/TAP.1971.1139990>
12. Справочник по специальным функциям / под ред. М. Абрамовица, И. Стигана. М.: Наука; Физматлит, 1979. 832 с.
13. Интегральное представление электромагнитного поля геометрически киральной структуры / В.А. Капитонов [и др.] // Физика волновых процессов и радиотехнические системы. 2012. Т. 15, № 4. С. 6–13.
14. Табаков Д.П. Тонкопроволочная модель фрактального симметричного вибратора на основе салфетки Серпинского // Радиотехника. 2015. № 2. С. 16–22.
15. Табаков Д.П., Морозов С.В., Ключев Д.С. Применение тонкопроволочного интегрального представления электромагнитного поля к решению задачи дифракции электромагнитных волн на проводящих телах // Физика волновых процессов и радиотехнические системы. 2022. Т. 25, № 2. С. 7–14. DOI: <https://doi.org/10.18469/1810-3189.2022.25.2.7-14>
16. Голуб Дж., Ван Лоун Ч. Матричные вычисления / пер. с англ. М.: Мир, 1999. 548 с.
17. Стрижков В.А. Математическое моделирование электродинамических процессов в сложных антенных системах // Математическое моделирование. 1989. Т. 1, № 8. С. 127–138. URL: <https://www.mathnet.ru/rus/mm/v1/i8/p127>
18. Интерактивная система просмотра системных руководств (ман-ов) // OpenNET. URL: <https://www.opennet.ru/man.shtml?topic=zgeev&category=3&russian=4>
19. LAPACK // Википедия. URL: <https://ru.wikipedia.org/wiki/LAPACK>
20. Ludick D.J., Jakobus U., Vogel M. A tracking algorithm for the eigenvectors calculated with characteristic mode analysis // The 8th European Conference on Antennas and Propagation (EuCAP 2014). 2014. P. 569–572. DOI: <https://doi.org/10.1109/EuCAP.2014.6901820>
21. Kalaba R., Spingarn K., Tesfatsion L. Individual tracking of an eigenvalue and eigenvector of a parameterized matrix // Nonlinear Analysis: Theory, Methods & Applications. 1981. Vol. 5, no. 4. P. 337–340. DOI: [https://doi.org/10.1016/0362-546X\(81\)90018-3](https://doi.org/10.1016/0362-546X(81)90018-3)

## Физика волновых процессов и радиотехнические системы 2023. Т. 26, № 1. С. 58–69

DOI 10.18469/1810-3189.2023.26.1.58-69  
УДК 537.862

Дата поступления 27 января 2023  
Дата принятия 27 февраля 2023

### Спектральные характеристики интегрального оператора внутренней задачи электродинамики для эллиптической рамочной структуры

Д.П. Табаков, А.Г. Майоров

Поволжский государственный университет телекоммуникаций и информатики  
443010, Россия, г. Самара,  
ул. Л. Толстого, 23

*Аннотация* – Статья посвящена анализу электродинамических свойств эллиптической рамочной структуры. С учетом двойной симметрии внутренняя задача для рассматриваемой структуры в рамках тонкопроволочного приближения сведена к четырем интегральным уравнениям Фредгольма первого рода, записанным относительно независимых токовых функций. Проведено исследование спектральных характеристик интегральных операторов соответствующих интегральных уравнений для различных значений электрической длины и коэффициента эллиптичности рамки. Показано, что собственные функции интегральных операторов при близких значениях указанных параметров имеют высокую степень корреляции и по форме близки к тригонометрическим функциям. Выявлены особенности частотной зависимости собственных значений интегральных операторов. Сделан вывод о резонансном характере этих зависимостей, что делает эллиптическую рамочную структуру во многом схожей с рассмотренными авторами ранее трубчатый вибратором и сферической спиральной частицей. Результаты, представленные в статье, способствуют формированию углубленного понимания процессов, протекающих в рассматриваемой структуре, а также служат ориентиром при построении аппроксимационных моделей решения внутренней задачи.

*Ключевые слова* – эллиптическая рамочная структура; рамочная антенна; интегральное представление электромагнитного поля; распределение тока; интегральное уравнение; собственные функции; собственные значения.

---

## Information about the Authors

**Dmitry P. Tabakov**, Doctor of Physical and Mathematical Sciences, professor of the Department of Physics, Povolzhskiy State University of Telecommunications and Informatics, Samara, Russia.

*Research interests:* electrodynamics, microwave devices and antennas, optics, numerical methods of mathematical modeling.

*E-mail:* illuminator84@yandex.ru

**Andrey G. Mayorov**, engineer of the Department of Radioelectronic Systems, Povolzhskiy State University of Telecommunications and Informatics, Samara, Russia.

*Research interests:* electrodynamics, microwave devices and antennas, numerical methods of mathematical modeling.

*E-mail:* andrey.mayorov.92@yandex.ru

## Информация об авторах

**Табаклов Дмитрий Петрович**, доктор физико-математических наук, профессор кафедры физики Поволжского государственного университета телекоммуникаций и информатики, г. Самара, Россия.

*Область научных интересов:* электродинамика, устройства СВЧ и антенны, оптика, численные методы математического моделирования.

*E-mail:* illuminator84@yandex.ru

**Майоров Андрей Геннадьевич**, инженер кафедры радиоэлектронных систем Поволжского государственного университета телекоммуникаций и информатики, г. Самара, Россия.

*Область научных интересов:* электродинамика, устройства СВЧ и антенны, численные методы математического моделирования.

*E-mail:* andrey.mayorov.92@yandex.ru